CHEMISTRY
A EUROPEAN JOURNAL

DOI: 10.1002/chem.201001695

Tri- and Tetraurea Piperazine Cyclophanes: Synthesis and Complexation Studies of Preorganized and Folded Receptor Molecules

Kari Raatikainen, N. Kodiah Beyeh, and Kari Rissanen*[a]

Abstract: A series of symmetrical tri- and tetrameric *N*-ethyl- and *N*-phenylurea-functionalized cyclophanes have been prepared in nearly quantitative yields (86–99%) from the corresponding tri- and tetraamino-functionalized piperazine cyclophanes and ethyl or phenyl isocyanates. Their conformational and complexation properties have been studied by single-crystal X-ray diffraction, variable-temperature NMR spectroscopy, and ESI-MS analysis. The rigid 27-membered trimeric cyclophane skeleton assisted by a seam of intramolecular hydrogen bonds results in a preorganized ditopic recognition site with an all-*syn* conformation of the urea moieties that, complemented by a lipophilic cavity of the cyclophane, binds molecular and ionic guests as well as ion pairs. The all-*syn* conformation persists in acidic conditions and the triprotonated triurea cyclophane binds an unprecedented anion pair, $H_2PO_4^-\cdots HPO_4^{2-}$, in the solid state. The tetra-*N*-ethylurea cyclophane is less rigid and demonstrates an induced-fit recognition of diisopropyl ether in the solid state. The guest was encapsulated within the lipophilic interior of a quasicapsule, formed by intramolecular hydrogen-bond-driven folding of the 36-membered cyclophane skeleton. In the gas phase, the essential role of the urea moieties in the binding was demonstrated by the formation of monomeric 1:1 complexes with K^+, TMA^+, and TMP^+ as well as the ion-pair complexes $[KI+K]^+$, $[TMABr+TMA]^+$ and $[TMPBr+TMP]^+$. In the positive-mode ESI-MS analysis, ion-pair binding was found to be more pronounced with the larger tetraurea cyclophanes. In the negative mode, owing to the large size of the binding site, a general binding preference towards larger anions, such as the iodide, over smaller anions, such as the fluoride, was observed.

Keywords: cyclophanes · host–guest systems · receptors · supramolecular chemistry · urea · X-ray diffraction

Introduction

Host–guest chemistry[1] has for a long time been one of the most intensively studied fields of supramolecular chemistry[2] yielding numerous novel host molecules capable of selective binding of specific molecular or ionic species through a multitude of noncovalent interactions. The design of hosts with such binding properties utilizes the principles of molecular recognition, which originate from the realm of biology, including factors like steric and interactional complementarity, the contact area, and the total number of common interaction sites between the host and the guest.[2] Among synthetic receptors, particular interest has for a long time focused on macrocyclic or macropolycyclic structures,[3,4] and more recently on rigid or semi-rigid macrocyclic receptor molecules that act as platforms onto which specific functional groups for noncovalent interactions can be attached.[5]

Urea-derivatized calixarenes are a particularly versatile and well-studied family of macrocyclic receptors that, through strong hydrogen bonds from the urea moiety,[6] show excellent halide-ion binding properties.[7] Additional sensing groups, such as ferrocene, have been attached to the urea moiety thereby enabling the detection of guests by optical and electrochemical methods.[8] Ditopic recognition by the calixarene π-donor cavity coupled with hydrogen-bonding urea moieties on the upper rim also provides an appropriate binding site for organic anions[9] or neutral hydrogen-bonding molecules[10] as well as amino acids.[11] This unique ditopic nature of urea-derivatized calixarenes has also been applied to ion-pair binding.[12]

The role of rigid molecular platforms is to preorganize the appropriately functional moieties to the desired spatial

[a] M. Sc. K. Raatikainen, Dr. N. K. Beyeh, Prof. K. Rissanen
Department of Chemistry, Nanoscience Center
University of Jyväskylä
Survontie 9, 40014 Jyväskylä (Finland)
Fax: (+35) 8142602672
E-mail: kari.t.rissanen@jyu.fi

Supporting information for this article is available on the WWW under http://dx.doi.org/10.1002/chem.201001695.

orientations for binding. Besides calixarenes[7–12] and resorcinarenes,[13–15] little attention has been paid to other types of macrocyclic platforms as cores for urea-functionalized receptors. One such less-studied family of compounds are piperazine-reinforced cyclophanes.[16] Piperazine, a cyclic bis-secondary diamine with a 1,4-diazacyclohexane skeleton, easily undergoes *N*-alkylation reactions with bis-functionalized spacer molecules to yield cyclic oligomers (piperazinophanes) under high-dilution conditions.[16,17] By using an appropriate spacer, the rigidity and cavity size can be tuned and suitable functional groups can be attached for further derivatization.[18] Recently we reported the synthesis of tri- and tetraamino piperazine cyclophanes **1** and **2** in which the aniline subunit was used as the functionalized spacer molecule (Scheme 1).[18] Structurally strained triamino cyclophane **1** has an all-*syn* conformation of the amino groups in the solid state. Larger and more flexible tetraamino cyclophane **2** folds into a very compact shell-like Pac-Man conformation due to a robust seam of circular intramolecular hydrogen bonds (Scheme 1) with an ability to form 1:1 inclusion complexes with suitably sized guest molecules.[18]

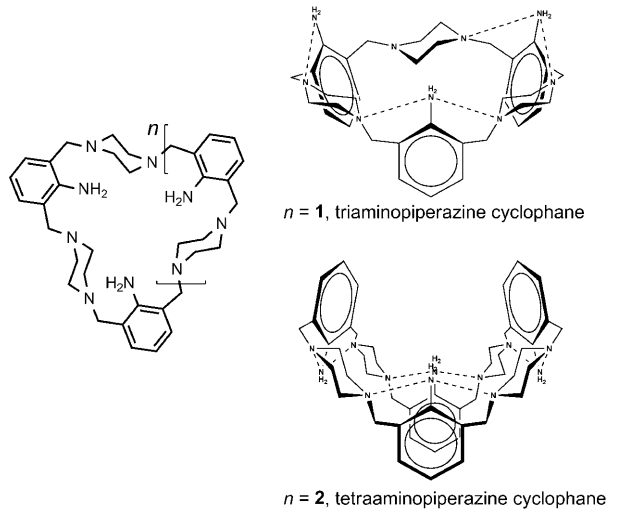

Scheme 1. The chemical structures and hydrogen-bond-driven conformations of **1** and **2**.

Herein we report a synthetic route to a small family of tri- and tetraurea piperazine cyclophanes with *N*-ethylurea (**3a** and **4a**) and *N*-phenylurea (**3b** and **4b**) as the functional groups. The trimeric cyclophane with urea groups in the all-*syn* conformation should provide a preorganized C_3-symmetric hydrogen-bonding donor site with six quite acidic hydrogen atoms for the binding of molecular or anionic guests. Flipping the urea groups through 180° would provide a similar site for cationic guests by binding to the urea carbonyl oxygen atoms. In the case of urea-functionalized tetrameric cyclophane, the seam of intramolecular hydrogen bonds would be lost, leading to greater conformational freedom. However, the binding process of a particular guest may require a built-in flexibility of the host whereby complexation can occur by an induced fit between the host and the guest.[2] The conformations and solid-state complexation properties of the title compounds were studied by variable-temperature NMR spectroscopy and single-crystal X-ray diffraction. The gas-phase host–guest behavior was studied by electrospray ionization (ESI) mass spectrometry in which the supramolecular complexes are formed without solvent or crystal-packing effects.[19]

Results and Discussion

Synthesis: The synthetic route to urea cyclophanes **3** and **4** is depicted in Scheme 2. Parent cyclophanes **1** and **2** have previously been prepared by the reaction of piperazine and 1,3-bis(bromomethyl)-2-nitrobenzene under high-dilution conditions followed by the reduction of the nitro groups with stannous(II) chloride in concentrated HCl solution.[18] The resulting amine-functionalized cyclophanes were dissolved in chloroform or dichloromethane and treated with an excess of ethyl or phenyl isocyanates. The isocyanates reacted readily with the amino groups to yield the corresponding tri- and tetraurea cyclophanes **3a**, **3b**, **4a**, and **4b** with yields of 93, 86, 93, and 99%, respectively (see the Experimental Section).

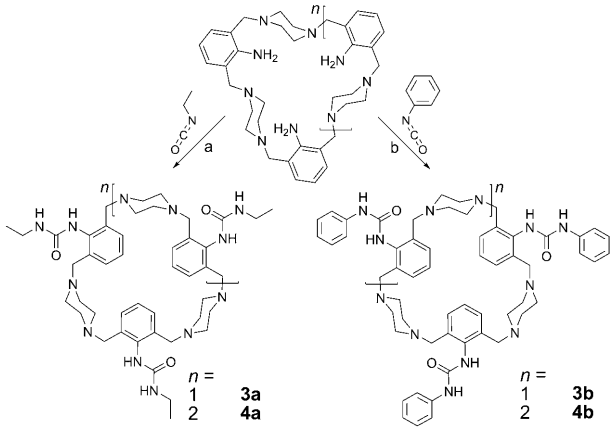

Scheme 2. Synthetic routes to **3a**, **3b**, **4a**, and **4b**.

X-ray crystallography: Crystals for X-ray diffraction analysis were obtained from methanol solutions of **3a**, **3b**, and **4a** (unfortunately no single crystals were obtained from **4b**) into which vaporized diisopropyl ether was allowed to diffuse at ambient temperature to yield crystal structures of **IIIa** (**3a**·$[MeOH]_2$·$[H_2O]$ [$i Pr_2O$]), **IIIb** (**3b**·$[MeOH]_3$), and **IV** (**4a**·$[MeOH]_6$·[$i Pr_2O$]). The binding properties of **3a** towards anionic guests was further investigated by co-crystallization with tetramethylphosphonium (TMP) chloride and bromide, tetramethylammonium (TMA) iodide, or tetrabutylammonium (TBA) dihydrogen phosphate in a molar ratio of 1:1. The crystallizations were performed in acetone solu-

tion by dropwise addition of methanol to first solubilize **3a** and then addition of the appropriate guest. X-ray-quality co-crystals were obtained only for the TMP chloride complex **IIIa**·[TMPCl] (**3a**·[TMPCl] · $[MeOH]_5$). For the other salts, attempts at co-crystallization in the presence of protic MeOH did not produce X-ray-quality crystals. To probe the effects of an acidic crystallization environment, **3a** was also crystallized from an ethanol solution carefully acidified (about 5% v/v) with concentrated phosphoric acid, which yielded crystals of **IIIa**·$[H_3PO_4]_2$ (**3a**·$[H_3PO_4]_2$·$[MeOH]_4$·$[H_2O]_4$).

IIIa crystallizes in a monoclinic crystal system in space group *C*2/*c*, the asymmetric unit containing one cyclophane, two methanol, one water, and one diisopropyl ether solvent molecule (Figure 1). As expected, the all-*syn* conformation[18] was retained and thus **IIIa** has an intramolecular cavity with a nearly perfect C_3-symmetric orientation of the urea groups. The geometry of the cavity, calculated from the centroid of the cyclophane (C_3, atoms N46, N52, and N55), gave angles of 126, 120, and 114° for N46···C_3···N52, N52···C_3···N58, and N58···C_3···N46, respectively. The corresponding C_3···N46, C_3···N52, and C_3···N58 distances, 4.71, 4.96, and 4.38 Å, reveal a relatively large cavity suitable for molecular guests or large tetrahedral anions like phosphate or sulfate. Molecular modeling[20] of **3a** and the PO_4^{3-} ion revealed strong hydrogen bonds and a nearly perfect spatial fit in the cavity formed by the three urea groups (Figure 2). The lower urea N–H moieties (N43, N55, and N49) form intramolecular hydrogen bonds with piperazine nitrogen atoms leading to a clockwise- or anti-clockwise-oriented (urea)N–H···N(piperazine) pattern, which additionally stabilizes the all-*syn* conformation (Table 1). Despite the identical cyclophane skeletons, the intramolecular cavity in the triamino cyclophane **1** is nearly closed due to its twisted conformation, whereas the ethylurea groups in **3a** make the conformation more open and symmetrical. Crystal packing reveals that molecules of **3a** form self-complementary dimers in which the ethylurea groups of the adjacent cyclophanes serve as guest moieties. The dimer is stabilized by N52–H···O57 and the solvent-mediated hydrogen-bond pattern (Figure 1b).

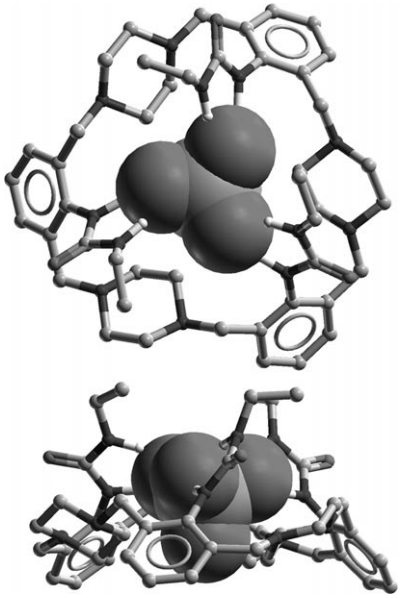

Figure 2. Molecular modeling[20a] of **3a** and the PO_4^{3-} ion reveals strong hydrogen bonds and a nearly perfect spatial fit into the cavity formed by the three urea groups.

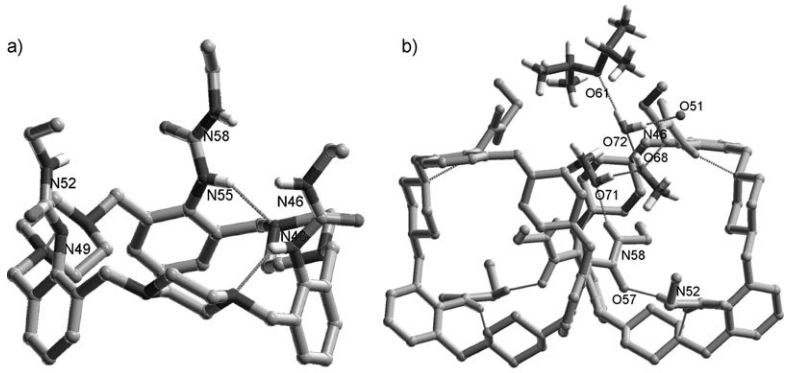

Figure 1. a) Crystal structure of **IIIa** with solvent molecules having been omitted for clarity and b) the self-complementary dimer structure of **IIIa** stabilized by intermolecular hydrogen bonds.

Crystalline host–guest complex **IIIa**·[TMPCl], obtained from a 1:1 mixture of **3a** and TMPCl, crystallizes in a triclinic unit cell in space group $P\bar{1}$. The all-*syn* conformation of the host is nearly identical to that of **IIIa** despite the completely different lattice environment. The chloride anion is complexed in a "corner" of the urea cavity and bound by four hydrogen bonds, one to the ethylurea group and three to MeOH solvent molecules (Figure 3). The remaining urea N–H donors N46 and N52 are also involved in hydrogen bonding with methanol molecules, which further extends the complex hydrogen-bond network (see Table 1). In the cavity of the cyclophane, two of the methanol solvents (O74 and O87) are positioned below and above the Cl^- guest. Owing to the three-fold molecular symmetry of the host, the other two methanol solvents (O67 and O78) and the Cl^- guest are equally disordered (occupancy 1/3) between three equivalent sites, that is, in the corners of the cavity. The TMP cation is trapped tightly into the intermolecular cavity that is formed by the phenylurea subunits of three adjacent cyclophanes (Figure 3b). In addition to the cation···π interactions, the oxygen atoms of the urea moieties point towards the positive phosphorus atom with O45···P61, O51···P61, and O57···P61 distances of 3.45, 3.51, and 3.50 Å, respectively.

Table 1. Specified hydrogen bonds for **IIIa**, **IIIa**·[TMPCl], **IIIb**, **IIIa**·$[H_3PO_4]_2$, and **IV**.

IIIa			**IIIa**·[TMPCl]		
Hydrogen bond	Length [Å]	Angle [°]	Hydrogen bond	Length [Å]	Angle [°]
N43–H···N8	2.880(3)	137(2)	N43–H···N39	2.851(4)	134(5)
N49–H···N22	2.834(3)	138(2)	N49–H···N11	2.893(3)	135(5)
N55–H···N36	2.838(3)	139(2)	N55–H···N25	2.861(4)	131(5)
N46–H···O68	3.066(5)	133(3)	N46–H···O78	2.757(9)	150(5)
O68–H···O72	2.739(5)	174	N52–H···O76	2.906(8)	168(6)
O71–H···O68	2.712(7)	161	N58–H···Cl73	3.307(5)	169(5)
O72–H···O61	2.969(4)	180	O74–H···Cl73	3.026(11)	178
N58–H···O71	2.853(6)	159	O87–H···Cl73	3.200(9)	177
N52–H···O57	2.838(3)	174(3)	O76–H···O74	2.684(14)	173
O72–H···O51	2.729(3)	179	O93–H···N22	2.880(6)	171
			O91–H···N36	2.900(4)	162
IIIb			**IIIa**·$[H_3PO_4]_2$		
Hydrogen bond	Length [Å]	Angle [°]	Hydrogen bond	Length [Å]	Angle [°]
N43–H···N8	2.893(3)	135(2)	N8–H···O64	2.590(8)	170
N53–H···N22	2.826(3)	134(2)	N22–H···O63	2.668(9)	151
N63–H···N36	2.816(3)	135(2)	N36–H···O65	2.649(8)	171
N66–H···O75	3.12(2)	172(2)	N43–H···N39	2.871(9)	113
O75–H···O81	2.67(2)	178	N49–H···N11	2.833(9)	110
O81–H···O79	2.788(7)	145	N55–H···N25	2.867(8)	111
O79–H···O55A	3.132(7)	161	N46–H···O79A	2.933(17)	172
O74–H···O79	2.832(4)	175(3)	N52–H···O74	2.893(12)	145
N46–H···O74	2.956(4)	165(3)	N58–H···O68	2.881(10)	161
			O62–H···O70	2.679(10)	175
			O69–H···O65	2.583(8)	166
			O72A–H···O68	2.630(14)	168
			O79A–H···O72A	2.819(18)	179
			O74–H···O70	2.664(10)	163

IV		
Hydrogen bond	Length [Å]	Angle [°]
N7–H···N77	2.835(4)	131(3)
N67–H···N74	2.873(3)	128(3)
N27–H···N34	2.794(3)	137(3)
N47–H···N37	2.823(3)	137(3)

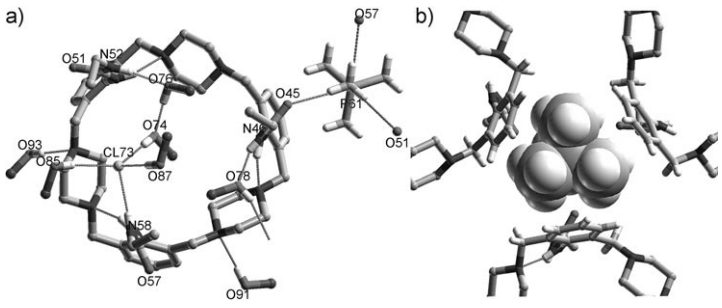

Figure 3. a) The hydrogen-bond interaction pattern in **IIIa**·[TMPCl], with only one position of the disordered Cl^- anions shown and the MeOH molecules bound to it. b) Partial view of the entrapment of the TMP cation between three adjacent cyclophanes.

The good steric and interactional complementarity of the cavity for the TMP^+ guest is illustrated in Figure 3b. This trigonal interaction geometry of the cation and the cyclophane extends to a two-dimensional honeycomb network.

IIIa·$[H_3PO_4]_2$ crystallizes in a trigonal unit cell in space group $P3_1$. Every second tertiary amino group, one in each piperazine moiety, is protonated resulting in a triprotonated cyclophane skeleton, which clearly reinforces the all-*syn* conformation of **3a** (Figure 4). The triprotonated state of the trimeric cyclophane is favored even in the presence of strong acids like HCl due to the small cyclic structure and limited conformational freedom.[21] The low-energy chair conformation[22] of the piperazine is not altered because the hydrogen atoms in the ammonium ion moieties point outwards from the macrocycle and the free electron pairs of the second piperazine nitrogen atoms are oriented inwards, appropriately acting as hydrogen-bond acceptors from the urea groups forming the seam of intramolecular hydrogen bonds (Figure 4a, Table 1). In addition to protonation, the phosphoric acid solution was used to study the role of the phosphate anion. As indicated by molecular modeling studies,[20] the size and shape of the binding cavity should favor tetrahedral anions and thus lead to phosphate binding. However, in **IIIa**·$[H_3PO_4]_2$, the anions are not fully deprotonated and are present as $H_2PO_4^-$ and HPO_4^{2-} ions. The dihydrogen phosphate and hydrogen phosphate ions form a [P=O···H–O–P] hydrogen-bonded anion pair (Figure 4a), which is partially included in the cavity formed by the urea moieties. The dihydrogen phosphate acts as an anchor for the binding. One of its P=O oxygen atoms (O68) is directly hydrogen-bonded to one urea group (N58) and through a methanol and water (O72A and O79A) hydrogen-bonded chain to a second urea group (N46). The second P=O oxygen atom (O70) is bound to the third urea group (N52) through a methanol (O74) molecule. The cyclophanes are packed into a 2D honeycomb network similar to that of **IIIa**·[TMPCl]. Now the hydrogen phosphate, which sits on the tip of the whole complex, fits exactly into the trigonal hole in the above layer and is bound to three cyclophanes through charge-assisted N8–H···O64, N22–H···O63, and N36–H···O65 hydrogen bonds (Figure 4b). The dihydrogen phosphate–hydrogen phosphate pair thus acts as an anchor between the off-set stacked 2D layers.

X-ray analysis of the phenylurea analogue **3b** (Figure 5) shows the monoclinic space group $P2_1/n$. The asymmetric unit contains one cyclophane and three methanol solvent molecules. In spite of the phenyl moieties, the structure of the host shows the same all-*syn* conformation with nearly identical intramolecular cavity diameters as in **3a**. The centroid (C_3) calculated from the atoms N46, N56, and N66 gives angles of 128, 116, and 116° for N46···C_3···N56, N56···C_3···N66, and N66···C_3···N46 and contact distances of 4.87, 4.87, and 4.25 Å for C_3···N46, C_3···N52, and C_3···N55, respectively. However, the N–C (C54–N56) bond of one urea group is rotated through 180°, which results in a horizontally oriented phenyl moiety that blocks the cavity. The all-*syn* conformation is stabilized by intramolecular hydrogen bonding between the lower N–H moiety of the urea groups and piperazine nitrogen atoms with similar clockwise or anticlockwise orientations of the N–H···N contacts to those in **IIIa** and **IIIa**·[TMPCl] (Table 1). Figure 6 shows the

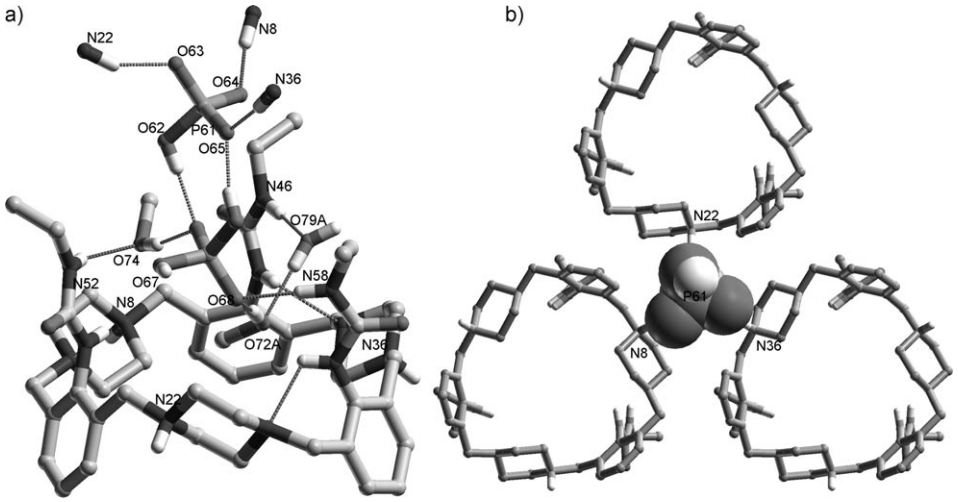

Figure 4. a) The hydrogen-bond interaction pattern in **IIIa**·$[H_3PO_4]_2$ that stabilizes the complex formed between the $H_2PO_4^-\cdots HPO_4^{2-}$ ion pair and **3a**. b) View of the 2D layer of cyclophanes showing entrapment of the hydrogen phosphate.

semblance to the Pac-Man conformation of the parent cyclophane **2**, yet is less compactly folded. Owing to its increased flexibility, the 36-membered cyclophane is actually wrapped around the diisopropyl ether guest, showing induced-fit binding with the flexible receptor, which results in a 1:1 capsule-type inclusion complex stabilized by N7–H···N(piperazine)N···H–N67 and N27–H···N(piperazine)N···H–N47 hydrogen-bond patterns (Table 1). The *N*-ethylurea groups point outwards from the capsule and the remaining upper rim of N–H donors form

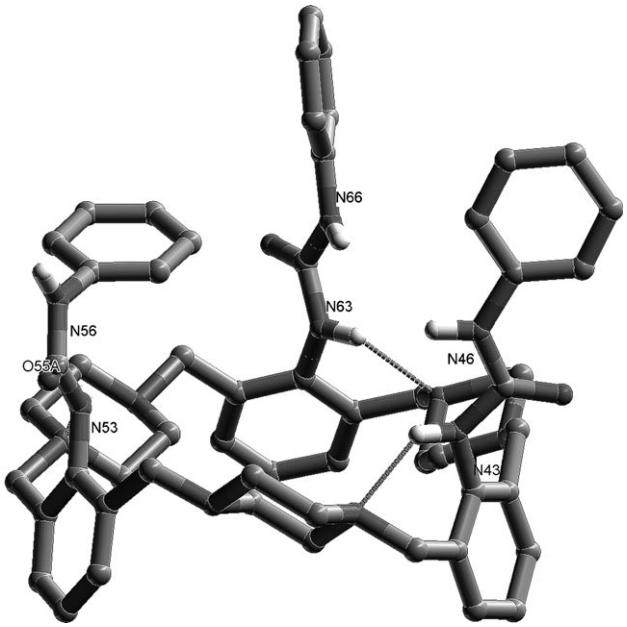

Figure 5. View of the crystal structure of **IIIb**. Solvent molecules have been omitted for clarity.

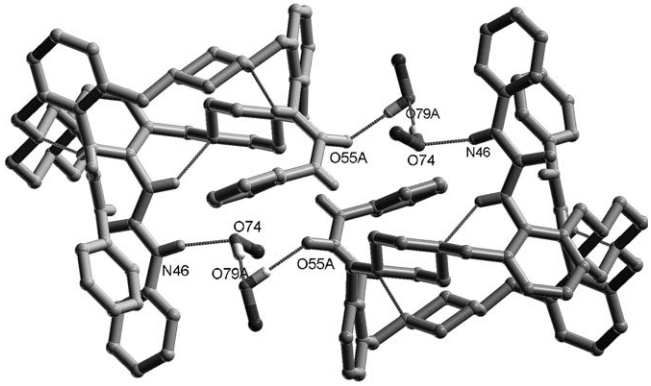

Figure 6. View of the methanol-mediated dimeric structure in **IIIb**.

centrosymmetric dimer of two cyclophanes linked by two N46–H···O74–H···O79A–H···O55A hydrogen-bonded chains involving two of the three methanol solvent molecules.

Although the all-*syn* conformation is characteristic of trimeric cyclophanes **1**, **3a**, and **3b**, the tetrameric analogues were expected to adopt the Pac-Man conformation of the parent cyclophane **2** or modified versions of this conformation. Unfortunately, only **4a** produced single crystals with structure **IV** (monoclinic, space group $P2_1/a$). The asymmetric unit consists of one cyclophane, one diisopropyl ether, and six methanol solvent molecules. Figure 7 shows that the cyclophane is folded into a conformation that has some re-

hydrogen-bond chain links through methanol solvent molecules to the adjacent complexes resulting in an extended 3D network.

Close examination of the X-ray structures of **1**, **2**, **IIIa**, **IIIb**, **IV**, and the previously studied acyclic analogues[18,23] revealed that intramolecular hydrogen bonding occurs when the donor hydrogen atom and the acceptor piperazine nitrogen atom are separated by five covalent bonds that form a cyclohexane-type ring through –N···H– interactions. In **4a**, only two of the piperazines are available for such hydrogen bonding. In the case of **2**, all four piperazine subunits are available to form the corresponding hydrogen bonds and thus a more compact conformation, the Pac-Man motif, dominates. When the diisopropyl ether guest was omitted from **IV**, a void volume[24] of 262 Å^3 was obtained, which gives a rough estimate of the size of the intramolecular cavity in **4a**. The intramolecular cavity in **IV** is more than twice as large as the cavity in the Pac-Man conformation of cyclophane **2**[18,21] (110 Å^3) and thus it can accommodate larger guests, such as diisopropyl ether with a molecular vol-

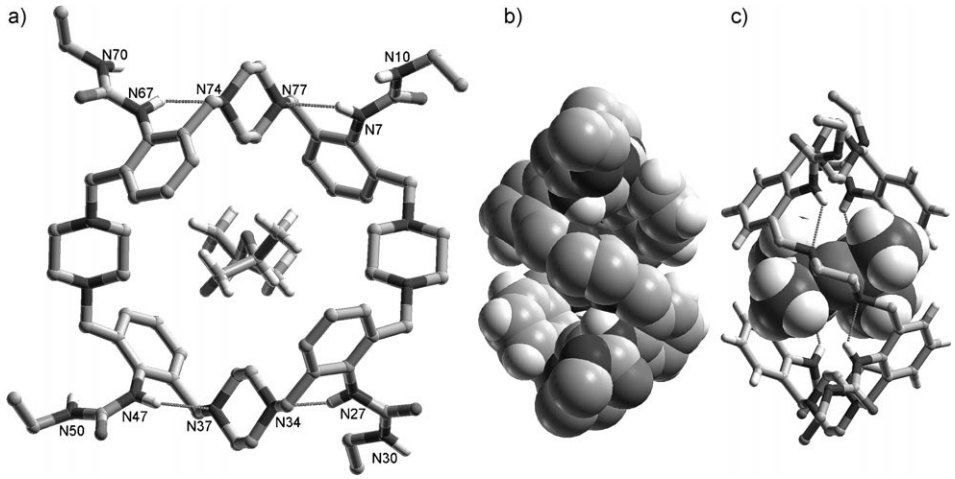

Figure 7. View of a) the crystal structure of **IV** (methanol solvent molecules have been omitted for clarity, b) empty **IV**, and c) the capsule-type complex with diisopropyl ether.

ume[20b] of 135 Å^3, which thus follows nicely the 55% rule by Mecozzi and Rebek.[25]

NMR spectroscopy: The ^{1}H NMR spectra of the cyclophanes **3a**,**b** and **4a**,**b** were recorded by using CD_3OD as solvent. The dynamic behavior of **3a** was examined further through variable-temperature NMR spectroscopy experiments. The spectra were recorded in the temperature range of 333 to 213 K and the effect of temperature on the spectra is illustrated in Figure 8. At 333 K, the CH_3 of the *N*-ethylurea groups appears as a triplet at $\delta = 1.14$ ppm and the CH_2 protons as a quartet at $\delta = 3.19$ ppm. The diastereotopic piperazine NCH_2 and benzylic $ArCH_2N$ protons are averaged to give broad singlets at $\delta = 2.30$ and 3.48 ppm, respectively. The aromatic protons appear as a triplet at $\delta = 7.07$ ppm and a doublet at $\delta = 7.25$ ppm. These sharp signals can be explained by the fast dynamics of the cyclophanes at higher temperatures. At 303 K, the signal of the benzylic protons is split into two resonances whereas the piperazine signal broadens and splits at lower temperatures. At 213 K, the signal for the diastereotopic piperazine protons is split into six signals. The dynamics, that is, the chair–chair interconversion and the ring rotation of the piperazines as well as flipping of the aryl units, at this temperature is clearly restricted and does not show any further changes below 213 K. In conclusion, the change in the dynamics at 213 K is suggested to arise from the intramolecular hydrogen-bond-stabilized conformation, which should finally lead to the all-*syn* conformation in the crystalline state. The insolubility of the cyclophanes in nonpolar solvents and most of the polar aprotic solvents rendered the anion-binding studies impossible in solution.

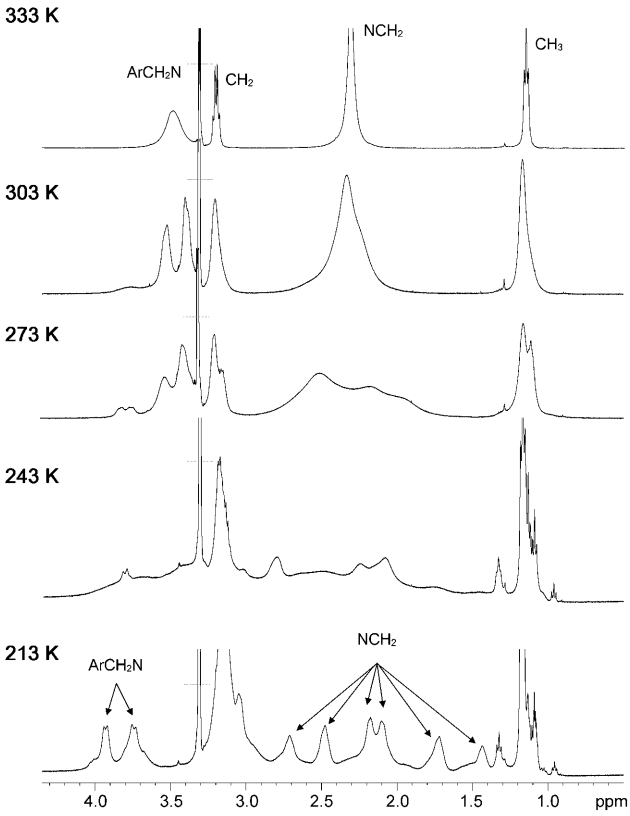

Figure 8. ^{1}H NMR spectra of **3a** in CD_3OD at different temperatures. At 333 K, the compound shows broad signals arising from diastereotopic piperazine protons that further broaden as the temperature reduces and finally split into six signals at 213 K. The benzyl protons also split into two separate doublets at 213 K, which indicates a rigid all-*syn* conformation. The single broad signal at higher temperatures can be explained by fast dynamics.

Mass spectrometry: The urea cyclophanes **3** and **4** can easily be ionized and transferred intact into the mass spectrometer by using the ESI technique with methanol as the spray solvent. Gas-phase complexation studies of the cyclophanes with potassium, TMA, and TMP salts were studied in the positive and negative ion modes. The mass spectra recorded in the complexation experiments with the tetrameric cyclophanes **2**, **4a**, and **4b** and potassium iodide (KI) are dominated by peaks that correspond to the protonated urea cyclophane and the potassium adducts (Figure 9). Urea groups that are correctly spatially situated are known to bind anions strongly and this is manifested in the binding of ion pairs in the gas phase, as evidenced by ions such as $[\mathbf{4a}+KI+K]^+$ (m/z 1301) and $[\mathbf{4b}+KI+K]^+$ (m/z 1493; Figure 9). The isotope patterns obtained in the experiments agree with those simulated on the basis of natural abundances. Complexation was not observed with the amino-functionalized reference cyclophane **2**, which signifies

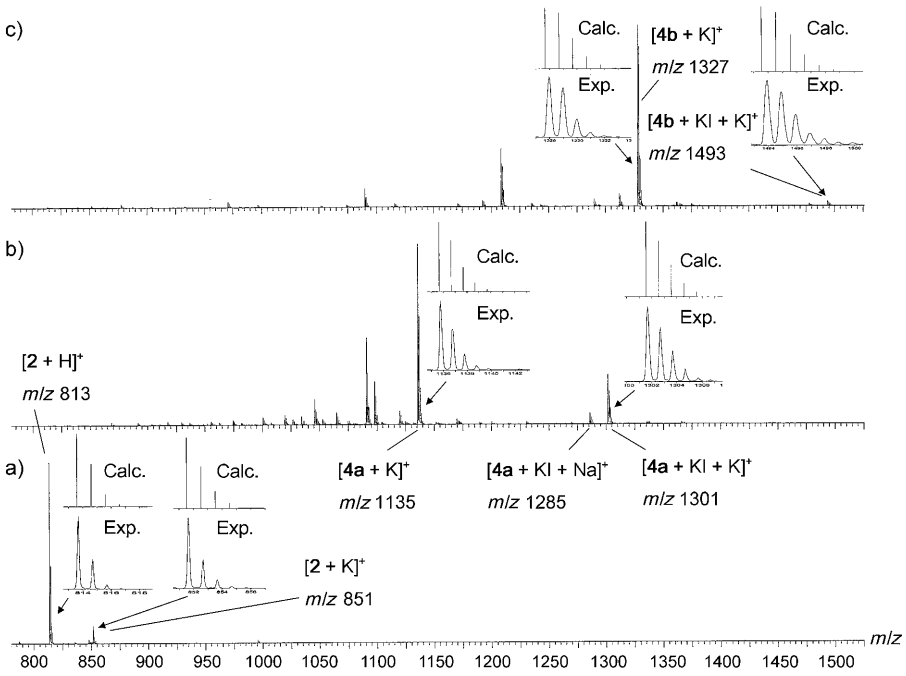

Figure 9. ESI-MS showing the complexation of KI with a) **2**, b) **4a**, and c) **4b**. Insets: Experimental and calculated isotope patterns.

the enhanced complexing ability of the urea-containing cyclophanes. Steric effects were also observed in the general complexing behavior of the receptors, as seen by the preference of ion-pair binding by the tetrameric cyclophanes over the trimeric cyclophanes. Ion-pair binding with the trimeric cyclophanes is generally weaker, as based on the observed intensities and peaks corresponding to $[\mathbf{3a}+\mathrm{HBr}+\mathrm{H}]^+$ (*m*/*z* 941) and $[\mathbf{3a}+\mathrm{HBr}+\mathrm{K}]^+$ (*m*/*z* 979). Protonated $[\mathbf{3a}_2+\mathrm{H}]^+$ (*m*/*z* 1646), $[\mathbf{3b}_2+\mathrm{H}]^+$ (*m*/*z* 1935), and potassium-containing $[\mathbf{3a}_2+\mathrm{K}]^+$ (*m*/*z* 1684) dimers are also detected in the gas phase (see the Supporting Information).

The amino-functionalized reference cyclophanes **1** and **2** did not show any gas-phase binding of the larger TMA and TMP salts. Addition of TMA and TMP salts to the reference compounds only led to signals corresponding to the protonated receptor. The urea groups are therefore essential for the binding of organic cations. Taking the complexation of the trimeric cyclophanes **1**, **3a**, and **3b** with TMPBr as an example, the mass spectra of the urea-containing cyclophanes show intense signals of $[\mathbf{3a}+\mathrm{TMP}]^+$ (*m*/*z* 913) and $[\mathbf{3b}+\mathrm{TMP}]^+$ (*m*/*z* 1057) corresponding to 1:1 complexes with the TMP cation (Figure 10). A similar trend was witnessed when TMA and TMP salts were mixed with the cyclophane hosts and the mixture injected into the mass spectrometer (see the Supporting Information).

Size selectivity was also observed in the complexing ability of the trimeric and tetrameric cyclophane receptors towards organic salts. Owing to their larger size, the tetrameric cyclophanes are better hosts for ion-pair binding. Taking the complexation of TMPBr as an example, signals corresponding to the ion-pair binding of the salts $[\mathbf{4a}+\mathrm{TMPBr}+\mathrm{TMP}]^+$ (*m*/*z* 1357) and $[\mathbf{4b}+\mathrm{TMPBr}+\mathrm{TMP}]^+$ (*m*/*z* 1549) were clearly detected in the mass spectra (Figure 11). A similar trend was observed when comparing the complexation of all the other organic salts with the cyclophane receptors (see the Supporting Information).

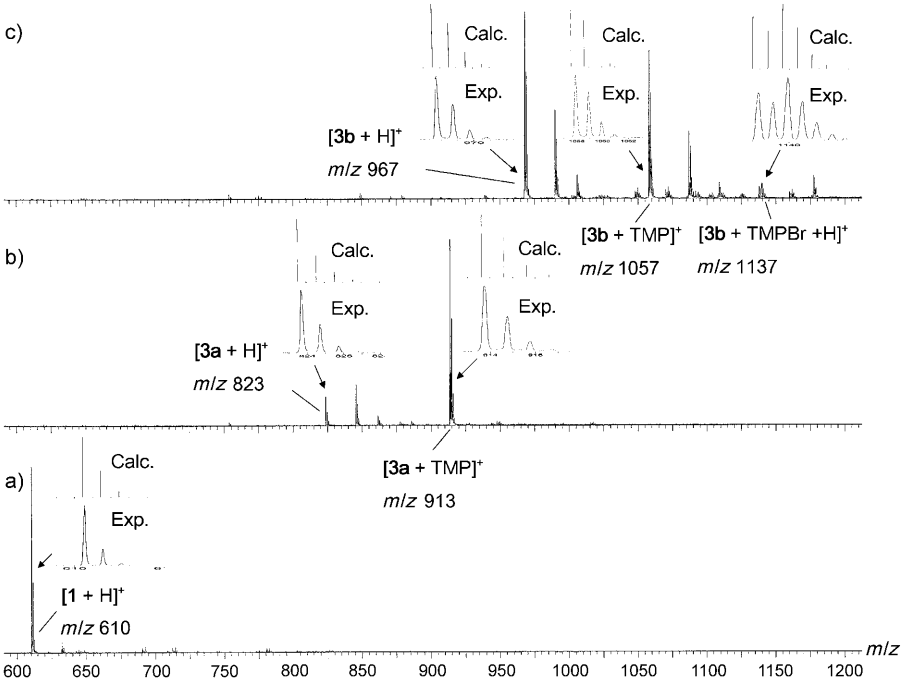

Figure 10. ESI-MS showing the complexation of TMPBr with a) **1**, b) **3a**, and c) **3b**. Insets: Experimental and calculated isotope patterns.

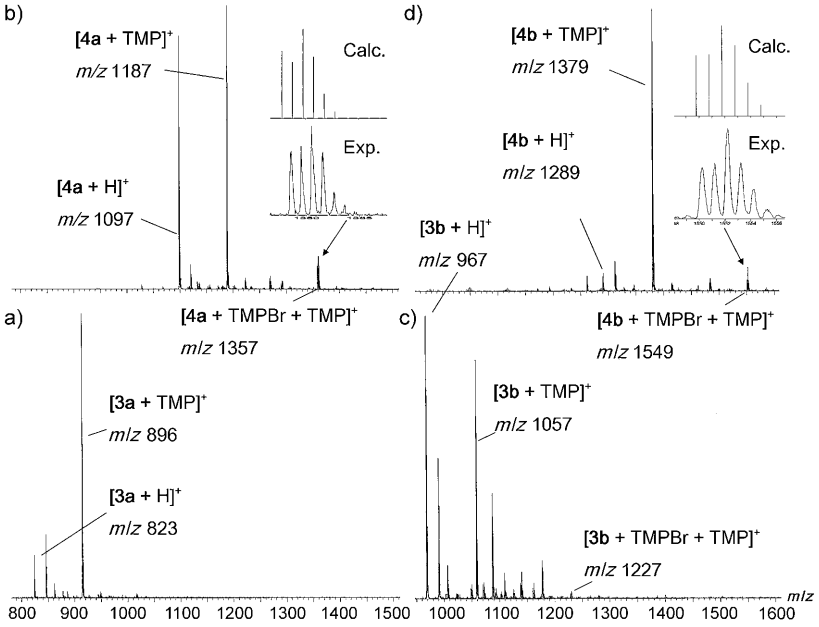

Figure 11. ESI-MS showing the complexation of TMPBr with a) **3a**, b) **4a**, c) **3b**, and d) **4b**. Insets: Experimental and calculated isotope patterns.

Taking the binding of KI by the tetrameric cyclophanes as an example in the negative ion mode, intense peaks corresponding to the binding of the iodide anion by the urea-containing hosts $[\mathbf{4a}+\mathrm{I}]^-$ (*m*/*z* 1223) and $[\mathbf{4b}+\mathrm{I}]^-$ (*m*/*z* 1415) were observed in the mass spectra whereas an intense signal corresponding to $[\mathbf{2}+\mathrm{HI}+\mathrm{I}]^-$ (*m*/*z* 1067) was observed with reference compound **2** (Figure 12). A similar trend was observed with all the other host/guest mixtures. A general size preference for halide-anion binding was observed. The lowest intensities were observed with fluorides whereas the highest intensities were observed with iodides (see the Supporting Information).

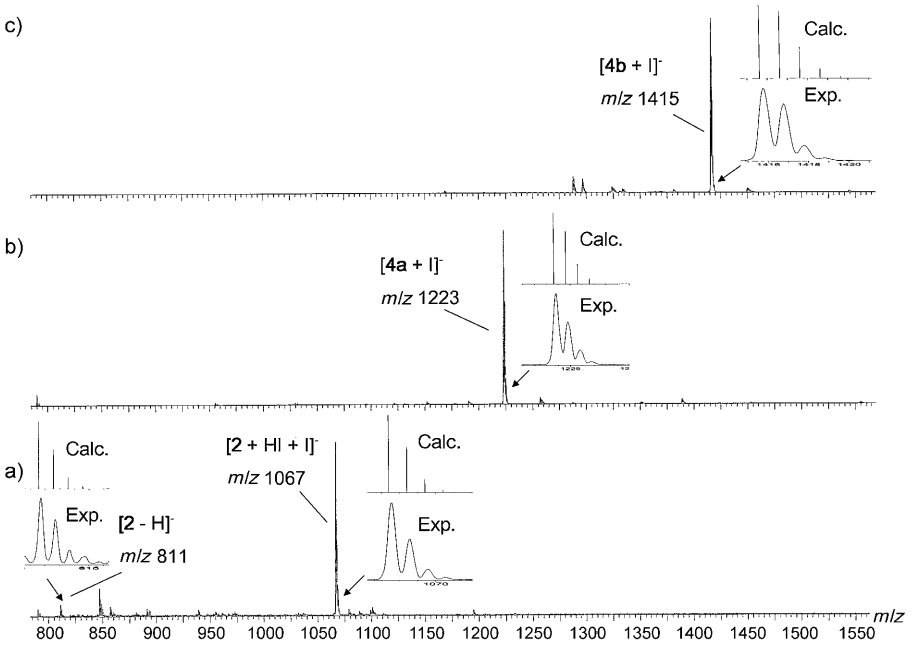

Figure 12. Negative ESI-MS showing the complexation of KI with a) **2**, b) **4a**, and c) **4b**. Insets: Experimental and calculated isotope patterns.

Conclusion

The reactions of alkyl or aryl isocyanates and amine-functionalized trimeric triamino and tetrameric tetraamino piperazine cyclophanes offer a straightforward route to the construction of new urea-functionalized cyclophanes (**3a**, **3b**, **4a**, and **4b**). Single-crystal structure determinations revealed that a proper spatial proximity of the hydrogen-bond donating and accepting sites on urea groups and piperazine moieties as well as the appropriately rigidified structures of the trimeric cyclophanes (**3a** and **3b**) leads to hydrogen-bond-stabilized all-*syn* conformations in which all urea groups are oriented on the same side of the cyclophane. The resulting cavity with a C_3-symmetric coordination sphere of strong hydrogen-bonding donors provides potential binding sites for molecular or anionic guests, which was demonstrated by molecular modeling studies and the co-crystallization of trimeric cyclophane and TMPCl (**IIIa**·[TMPCl]). The less-strained structures of the tetrameric cyclophanes with less preorganized orientations of the urea binding moieties provide a large and lipophilic intramolecular cavity. In the crystalline state, **4a** forms a hydrogen-bond-stabilized capsule-like inclusion complex with diisopropyl ether with excellent steric complementarity.

The host–guest properties of the cyclophanes towards potassium, tetramethylammonium, and tetramethylphosphonium salts were also investigated in the gas phase by ESI mass spectrometric techniques. The larger tetrameric cyclophane

hosts (**4a** and **4b**) are the most suitable for ion-pair binding, which was mainly observed in the positive ion mode. In the negative ion mode, a general preference was observed for the anion binding of larger anions, such as iodide, over smaller anions, like fluoride.

Experimental Section

General remarks: All chemicals and solvents were reagent grade, purchased commercially and used as such. Cyclophanes **1** and **2** were synthesized following previously reported procedures.[18] ^{1}H and ^{13}C NMR spectra were recorded with a Bruker Avance DRX 500 FT NMR spectrometer operating at 500 MHz for ^{1}H NMR spectra and at 126 MHz for ^{13}C NMR spectra. All spectra were recorded in CD_3OD at 60 °C unless otherwise stated (using the center solvent peak at $\delta = 3.31$ ppm and at $\delta = 49.15$ ppm of TMS as internal references for the ^{1}H and ^{13}C NMR spectra, respectively). Mass spectra were obtained by using a Micromass (ESI-TOF) spectrometer. Elemental analyses were carried out by using a VariolEL instrument from Elementar Analysensysteme. Melting points were measured with a Mettler Toledo FP62 apparatus.

X-ray crystallography:[26] Suitable crystals of **IIIa**, **IIIa**·[TMPCl], **IIIa**·$[H_3PO_4]_2$, **IIIb**, and **IV** for single-crystal X-ray diffraction analysis were selected and analyses were performed by using a Bruker Kappa Apex II diffractometer with graphite-monochromatized $Mo_{K\alpha}$ ($\lambda = 0.71073$ Å) radiation for **IIIa**, **IIIa**·[TMPCl], **IIIa**·$[H_3PO_4]_2$, and **IV** and $Cu_{K\alpha}$ ($\lambda = 1.54184$ Å) radiation for **IIIb**. COLLECT software[27] was used for the data measurement and DENZO-SMN[28] for the processing. Structures were solved by direct methods with SIR97[29] and refined by full-matrix least-squares methods with WinGX software,[30] which utilizes the SHELXL-97 module.[31] All C–H hydrogen positions were calculated in idealized positions by using a riding atom model after anisotropic refinement of all non-hydrogen atoms in the structure. All N–H hydrogen atoms were located from the electron density map and refined with restrained bond distances using isotropic displacement parameters of 1.2 U_{eq} of the attached nitrogen atom. Most of the O–H hydrogen atoms were located from the electron density map and refined as a rotating group by using the same (1.2 U_{eq}) isotropic displacement parameters.

Owing to the low data resolution in **IIIa**·$[H_3PO_4]_2$, the N–H and O–H hydrogen atoms could not be located from the electron density map and hence they were calculated with the riding atom model to give the idealized hydrogen bond positions. The protonated piperazine nitrogen atoms were deduced from the close proximity of phosphate anions. In the case of **IIIa**, the water O–H hydrogen atoms could not be located from the electron density map but instead deduced from the idealized hydrogen bond positions and refined with the riding atom model. Residual electron density in **IIIa** and **IIIa**·[TMPCl], due to the unresolved solvent molecule disorder, was treated by PLATON squeeze.[24] Detailed crystallographic data for all structures are summarized in Table 2.

Mass spectrometry: The mass spectrometric studies were performed with a micromass LCT ESI-TOF instrument equipped with a *Z* geometry electrospray ion source. Samples were introduced into the source as methanol solution mixtures of the hosts and the salts at flow rates of 30 μL min^{-1}. A constant spray and the highest intensities were achieved with a capillary voltage of 4200–4500 V at a source temperature of 80 °C and a dissolvation temperature of 120 °C with a sample cone voltage of 5–60 V. Because the instrument does not permit MS/MS experiments, the fragmentation behavior of the samples was examined by in-source fragmentation-induced collisions with the gas molecules present in the ion source. For this purpose, the ions were accelerated to different kinetic energies by tuning the sample cone voltage to different settings. At low voltage, the ions are not significantly accelerated and undergo fragmentation only to a minor extent upon collision with the surrounding gas molecules. With a high sample cone voltage, the ions approach the sample cone at a higher velocity and collisions with the surrounding gas lead to more pronounced fragmentations.

Synthesis

General procedure for the preparation of 3a, 3b, 4a, and 4b: Ethyl or phenyl isocyanate was added to a solution of the cyclophane in chloroform or dichloromethane and the resulting mixture was stirred for 24 h at ambient temperature under nitrogen atmosphere. A bulky white precipitate of the ethylurea-substituted derivative was collected by filtration and washed with copious amounts of dichloromethane and diethyl ether. The phenylurea-substituted derivatives were obtained from the reaction mixture as colorless crystals when mixed with acetonitrile and collected by filtration.

3a: Cyclophane **1** (64.0 mg, 0.105 mmol), chloroform (0.65 mL), and ethyl isocyanate (0.037 mL, 0.472 mmol). Yield: 80 mg, 93 %; m.p. 222 °C;

Table 2. Crystallographic data for **IIIa**, **IIIa**·[TMPCl], **IIIa**·$[H_3PO_4]_2$, **IIIb**, and **IV**.

Crystal	**IIIa**	**IIIa**·[TMPCl]	**IIIa**·$[H_3PO_4]_2$	**IIIb**	**IV**
formula	$C_{51.30}H_{85.20}N_{12}O_{6.70}$	$C_{54}H_{98}ClN_{12}O_8P$	$C_{49}H_{96}N_{12}O_{19}P_2$	$C_{60}H_{78}N_{12}O_6$	$C_{71}H_{124}N_{16}O_{11}$
space group	*C*2/*c*	$P\bar{1}$	$P3_1$	$P2_1/n$	$P2_1/a$
a [Å]	28.5875(4)	15.7470(4)	13.9673(5)	18.6515(3)	15.9913(4)
b [Å]	16.1250(2)	15.9632(4)	13.9673(5)	12.8679(2)	15.8319(3)
c [Å]	28.1471(4)	16.0730(4)	29.2072(12)	25.8001(4)	32.4111(7)
α [°]	90	66.7102(13)	90	90	90
β [°]	116.4560(10)	78.8183(13)	90	107.1990(10)	101.8160(10)
γ [°]	90	61.1826(15)	120	90	90
V [Å^3]	11616.3(3)	3251.49(14)	4934.5(3)	5915.28(16)	8031.7(3)
Z	8	2	3	4	4
T [K]	123(2)	123(2)	123(2)	173(2)	123(2)
ρ_{calcd} [g cm^{-3}]	1.118	1.134	1.231	1.194	1.139
μ [mm^{-1}]	0.075	0.139	0.140	0.632	0.078
θ_{max} [°]	25.0	27.5	25.0	63.47	27.5
θ comp. [%]	0.995	0.992	0.995	0.988	0.998
no. reflections	10187	14822	9522	9568	18436
parameters	718	768	690	774	938
restraints	58	24	626	16	0
R_1 [$I > 2\sigma(I)$]	0.0639	0.0825	0.0967	0.0621	0.0772
wR_2 [$I > 2\sigma(I)$]	0.1567	0.1965	0.2406	0.1619	0.1558
GOF on F^2	1.047	1.043	1.024	1.065	1.09
ΔF_{max} [e Å^{-3}]	0.435	0.811	0.704	0.452	0.669
ΔF_{min} [e Å^{-3}]	−0.334	−0.593	−0.415	−0.239	−0.353

^{1}H NMR (500 MHz, CD_3OD): $\delta = 1.15$ (t, $^3J = 6.95$ Hz, 9H), 2.31 (s, 24H), 3.21 (q, $^3J = 7.00$ Hz, 6H), 3.49 (s, 12H), 7.07 (t, $^3J = 7.13$ Hz, 3H), 7.26 ppm (d, $^3J = 7.61$, 6H); ^{13}C NMR (126 MHz, CD_3OD): $\delta = 15.85$, 36.49, 53.77, 60.61, 126.37, 130.62, 134.20, 138.56, 159.38 ppm; elemental analysis calcd (%) for $C_{45}H_{66}N_{12}O_3 \cdot CHCl_3$: N 19.5, C 63.1, H 7.8; found: N 19.7, C 63.1, H 7.8.

3b: Cyclophane **1** (50.0 mg, 0.082 mmol), dichloromethane (0.50 mL), and phenyl isocyanate (0.0401 mL, 0.369 mmol). Yield: 68 mg, 86%; m.p. 218°C; ^{1}H NMR (500 MHz, CD_3OD): $\delta = 2.16$ (s, 24H), 3.37 (d, $^3J = 13.25$ Hz, 6H), 3.57 (d, $^3J = 12.96$ Hz, 6H), 7.04–7.40 ppm (m, 24H); ^{13}C NMR (126 MHz, CD_3OD): $\delta = 53.77$, 60.85, 123.08, 125.47, 126.35, 130.12, 130.50, 134.01, 138.09, 140.52, 156.91 ppm; elemental analysis calcd (%) for $C_{57}H_{66}N_{12}O_3 \cdot CH_2Cl_2$: N 17.0, C 69.6, H 6.8; found: N 17.2, C 69.8, H 6.8.

4a: Cyclophane **2** (60 mg, 0.074 mmol), dichloromethane (0.60 mL), and ethyl isocyanate (0.035 mL, 0.443 mmol). Yield: 75 mg, 93%; m.p. 211°C; ^{1}H NMR (500 MHz, 30°C, CD_3OD): $\delta = 1.12$ (t, $^3J = 7.20$ Hz, 12H), 2.41 (s, 32H), 3.18 (q, $^3J = 7.20$ Hz, 8H), 3.50 (s, 16H), 7.11 (t, $^3J = 7.55$ Hz, 4H), 7.28 ppm (d, $^3J = 7.60$, 8H); ^{13}C NMR (126 MHz, CD_3OD): $\delta = 15.93$, 36.39, 49.66, 60.53, 126.73, 130.58, 135.41, 138.22, 159.33 ppm; elemental analysis calcd (%) for $C_{60}H_{88}N_{16}O_4 \cdot CH_2Cl_2$: N 19.9, C 64.4, H 7.9; found: N 19.8, C 64.2, H 8.0.

4b: Cyclophane **2** (50 mg, 0.061 mmol), dichloromethane (0.50 mL), and phenyl isocyanate (0.0435 mL, 0.369 mmol). Yield: 78 mg, 98%; m.p. 206°C; ^{1}H NMR (500 MHz, 30°C, CD_3OD): $\delta = 2.30$ (s, 32H), 3.49 (s, 16H), 7.00 (t, $^3J = 7.35$ Hz, 4H), 7.11 (t, $^3J = 7.61$ Hz, 4H), 7.25–7.7.30 (m, 16H), 7.39 ppm (d, $^3J = 7.55$ Hz, 8H); ^{13}C NMR (126 MHz, CD_3OD): $\delta = 53.96$, 60.96, 122.04, 124.83, 126.58, 129.68, 130.42, 134.65, 137.65, 140.78, 156.41 ppm; elemental analysis calcd (%) for $C_{76}H_{88}N_{16}O_4 \cdot CH_2Cl_2$: N 16.8, C 69.0, H 6.7; found: N 16.9, C 69.0, H 6.8.

Acknowledgements

Financial support from the Academy of Finland (no. 212588 and 218325) and the National Graduate School of Organic Chemistry and Chemical Biology is gratefully acknowledged. We thank Spec. Lab. Technician Reijo Kauppinen for his help in recording the NMR spectra.

[1] D. J. Cram, *Science* **1988**, *240*, 760.
[2] J-M. Lehn, *Supramolecular chemistry—Scope and Perspectives*, Wiley-VCH, Weinheim, **1995**.
[3] a) C. J. Pedersen, *J. Am. Chem. Soc.* **1967**, *89*, 7017; b) C. J. Pedersen, *J. Am. Chem. Soc.* **1967**, *89*, 2495.
[4] a) J.-M. Lehn, *Acc. Chem. Res.* **1978**, *11*, 49; b) J.-M. Lehn, *Pure Appl. Chem.* **1978**, *50*, 871.
[5] a) D. Coquière, S. Le Gac, U. Darbost, O. Seneque, I. Jabin, O. Reinaud, *Org. Biomol. Chem.* **2009**, *7*, 2485; b) C.-H. Lee, H. Miyaji, D.-W. Yoon, J. L. Sessler, *Chem. Commun.* **2008**, 24; c) V. Arora, H. M. Chawla, S. P. Singh, *ARKIVOC* **2007**, 172.
[6] M. C. Etter, T. W. Panunto, *J. Am. Chem. Soc.* **1988**, *110*, 5896.
[7] a) M. Menand, I. Jabin, *Org. Lett.* **2009**, *11*, 673; b) J. N. Babu, V. Bhalla, M. Kumar, R. K. Puri, R. K. Mahajan, *New J. Chem.* **2009**, *33*, 675; c) J. Babu, B. Nagendra; K. Vandana; M. R. K. Manoj; R. K. Puri, *Tetrahedron Lett.* **2008**, *49*, 2772; K. Vandana; M. R. K. Manoj; R. K. Puri, *Tetrahedron Lett.* **2008**, *49*, 2772; d) J. Budka, P. Lhotak, V. Michlova, I Stibor, *Tetrahedron Lett.* **2001**, *42*, 1583; e) J. Scheerder, R. H. Vreekamp, J. F. J. Engbersen, W. Verboom, J. P. M. van Duynhoven, D. N. Reinhoudt, *J. Org. Chem.* **1996**, *61*, 3476; f) J. Scheerder, J. P. M. van Duynhoven, J. F. J. Engbersen, D. N. Reinhouldt, *Angew. Chem.* **1996**, *109*, 1172; *Angew. Chem. Int. Ed. Engl.* **1996**, *35*, 1090; g) J. Scheerder, M. Fochi, J. F. J. Engbersen, D. N. Reinhoudt, *J. Org. Chem.* **1994**, *59*, 7815.
[8] a) E. Métay, M. C. Duclos, S. Pellet-Rostaing, M. Lemaire, J. Schulz, R. Kannappan, C. Bucher, E. Saint-Aman, C. Chaix, *Eur. J. Org. Chem.* **2008**, 4304; b) E. Métay, M. C. Duclos, S. Pellet-Rostaing, M. Lemaire, J. Schulz, R. Kannappan, C. Bucher, E. Saint-Aman, C. Chaix, *Eur. J. Org. Chem.* **2008**, 4304; c) B. Schazmann, N. Alhashimy, D. Diamond, *J. Am. Chem. Soc.* **2006**, *128*, 8607; d) A. J. Evans, S. E. Matthews, A. R. Cowley, P. D. Beer, *Dalton Trans.* **2003**, 4644.
[9] T. Haino, M. Nakamura, N. Kato, M. Hiraoka, Y. Fukazawa, *Tetrahedron Lett.* **2004**, *45*, 2281.
[10] A. Arduini, E. Brindani, G. Giorgi, A. Pochini, A. Secchi, *Tetrahedron* **2003**, *59*, 7587.
[11] a) F. P. Ballistreri, A. Notti, S. Pappalardo, M. F. Parisi, P. I. Pisagatti, *Org. Lett.* **2003**, *5*, 1071; b) A. V. Yakovenko, V. I. Boyko, V. L. Kalchenko, L. Baldini, A. Casnati, F. Sansone, R. Ungaro, *J. Org. Chem.* **2007**, *72*, 3223.
[12] a) M. Hamon, M. Menand, S. Le Gac, M. Luhmer, V. Dalla, I Jabin, *J. Org. Chem.* **2008**, *73*, 7067; b) N. Pelizzi, A. Casnati, A. Friggeri, R. Ungaro, *J. Chem. Soc. Perkin Trans. 2* **1998**, 1307.
[13] a) D. C. Gutsche, *Acc. Chem. Res.* **1983**, *16*, 161; b) P. Timmerman, W. Verboom, D. Reinhoudt, *Tetrahedron* **1996**, *52*, 2663.
[14] a) D. M. Rudkevich, G. Hilmersson, J. Rebek Jr. , *J. Am. Chem. Soc.* **1998**, *120*, 12216; b) A. Shivanyuk, K. Rissanen, S. K. Korner, D. M. Rudkevich, J. Rebek, Jr., *Helv. Chim. Acta* **2000**, *83*, 1778; c) A. R. Renslo, F. C. Tucci, D. M. Rudkevich, J. Rebek, Jr., *J. Am. Chem. Soc.* **2000**, *122*, 4573; d) R. J. Hooley, J. Rebek, Jr., *J. Am. Chem. Soc.* **2005**, *127*, 11904; e) A. Lledó, J. Rebek, Jr., *Chem. Commun.* **2010**, *46*, 1637.
[15] a) D. Ajami, J. Rebek, Jr., *J. Org. Chem.* **2009**, *74*, 6584; b) L. R. MacGillivray, J. L. Atwood, *Nature* **1997**, *389*, 469; c) L. Avram, Y. Cohen, *J. Am. Chem. Soc.* **2004**, *126*, 11556; d) K. Kobayashi, K. Ishii, S. Sakamoto, T. Shirasaka, K. Yamaguchi, *J. Am. Chem. Soc.* **2003**, *125*, 10615; e) F. Fochi, P. Jacopozzi, E. Wegelius, K. Rissanen, P. Cozzini, E. Marastoni, E. Fisicaro, P. Manini, R. Fokkens, E. Dalcanale, *J. Am. Chem. Soc.* **2001**, *123*, 7539; f) G. V. Oshovsky, D. N. Reinhoudt, W. Verboom, *J. Am. Chem. Soc.* **2006**, *128*, 5270.
[16] a) K. Rissanen, K. J. Huuskonen, A. Koskinen, *J. Chem. Soc. Chem. Commun.* **1993**, 771; b) K. Rissanen, J. Breitenbach, J. Huuskonen, *J. Chem. Soc. Chem. Commun.* **1994**, 1265; c) J. Huuskonen, J. Schulz, K. Rissanen, *Liebigs Ann.* **1995**, 1515; d) J. Huuskonen, J. Schulz, E. Kolehmainen, K. Rissanen, *Chem. Ber.* **1994**, *127*, 2267; e) J. Huuskonen, K. Rissanen, *Liebigs Ann.* **1995**, 1611.
[17] a) R. Gleiter, K. Hovermann, F. Rominger, T. Oeser, *Eur. J. Org. Chem.* **2001**, 725; b) K. E. Krakowiak, J. S. Bradshaw, W. Jiang, N. K. Dalley, G. Wu, R. M. Izatt, *J. Org. Chem.* **1991**, *56*, 2675.
[18] K. Raatikainen, J. Huuskonen, E. Kolehmainen, K. Rissanen, *Chem. Eur. J.* **2008**, *14*, 3297.
[19] a) M. Przybylski, M. O. Glocker, *Angew. Chem.* **1996**, *108*, 878; *Angew. Chem. Int. Ed. Engl.* **1996**, *35*, 806; b) J. S. Brodbelt, *Int. J. Mass Spectrom.* **2000**, *200*, 57; c) C. A. Schalley, *Int. J. Mass Spectrom.* **2000**, *194*, 11; d) C. B. Lebrilla, *Acc. Chem. Res.* **2001**, *34*, 653; e) C. A. Schalley, *Mass Spectrom. Rev.* **2001**, *20*, 253.
[20] SPARTAN 08, Wavefunction Inc., 18401 Von Karman Ave, Suite 370, Irvine; a) MMFF b) DFT, B3LYP, HF 6-31G*.
[21] K. Raatikainen, K. Rissanen, *Cryst. Growth Des.* **2010**, *10*, 3638.
[22] N. L Allinger, J. G. D. Carpenter, F. M. Karkowski, *J. Am. Chem. Soc.* **1965**, *87*, 1232.
[23] a) S. Mukhopadhyay, D. Mandal, P. B. Chatterjee, C. Desplanches, J.-P. Sutter, R. J. Butcher, M. Chaudhury, *Inorg. Chem.* **2004**, *43*, 8501; b) K. Kubono, K. Yokoi, *Acta Crystallogr. Sect. A* **2007**, *63*, 535; c) M. Kuppayee, D. Kumaran, M. N. Ponnuswamy, M. Kandaswamy, M. V. Jayanthi, K. Chinnakali, H.-K. Fun, *Acta Crystallogr. Sect. A* **1999**, *55*, 2147; d) K. Kubono, Y. Tsuno, K. Tani, K. Yokoi, *Acta Crystallogr. Sect. A* **2008**, *64*, o2309; e) S. Mohanty, D. Suresh, M. S. Balakrishna, J. T. Mague, *Tetrahedron* **2008**, *64*, 240; f) R. Thirumurugan, S. S. S. Raj, G. Shanmugam, H.-K. Fun, K. Chinnakali, S. Chantrapromma, M. Marappan, M. Kandaswamy, *Acta Crystallogr. Sect. A* **1998**, *54*, 780; g) S. Loukiala, J. Ratilainen, J. Valkonen, K. Rissanen, *Acta Chem.Scand.* **1997**, *51*, 1162.
[24] A. L. Spek, *J. Appl. Crystallogr.* **2003**, *36*, 7.
[25] S. Mecozzi, J. Rebek, Jr., *Chem. Eur. J.* **1998**, *4*, 1016.
[26] CCDC-780772, -780773, -780774, -780775 and -780772 contain the supplementary crystallographic data for this paper. These data can

be obtained free of charge from The Cambridge Crystallographic Data Centre via www.ccdc.cam.ac.uk/data_request/cif.
[27] COLLECT, R. W. Hooft, Nonius BV, Delft (The Netherlands), **1998**.
[28] Z. Otwinowski W. Minor, *Methods Enzymol.* **1997**, *276*, 307.
[29] A. Altomare, M. C. Burla, M. Camalli, G. L. Cascarano, C. Giacovazzo, A. Guagliardi, A. G. G. Moliterni, G. Polidori R. Spagna, *J. Appl. Crystallogr.* **1999**, *32*, 115.
[30] L. J. Farrugia, *J. Appl. Crystallogr.* **1999**, *32*, 837.
[31] G. M. Sheldrick, University of Göttingen (Germany), **1998**.

Received: June 15, 2010
Revised: September 10, 2010
Published online: November 12, 2010

